the AP diameter of the spinal cord, and was observed only in the gray matter and part of the anterior funiculus. At 20% compression, the stress on the gray matter and anterior funiculus was slightly increased. At 30% compression, the stress on the spinal cord was increased and high stresses were observed in the gray matter and the anterior, lateral and posterior funiculi. However, the stress was not increased on the posterior funiculus of the non-compressed side (Fig. 3C).

A compression of 62.5% of the length of the transverse diameter of the spinal cord with a rigid flat plate resulted in very low stresses when the degree of compression was 10% of the AP diameter of the spinal cord; the stress was only slightly increased in both anterior funiculi. At 20% compression, the stress increased in the gray matter and the anterior funiculus on the compressed side. At 30% compression, the stress on the spinal cord was increased and high stresses were observed in the gray matter and anterior funiculi of both sides, the lateral funiculus of the compressed side and both posterior funiculi. The stress was not increased in the lateral funiculus of the non-compressed side (Fig. 3D).

Under compression of 75% of the length of the transverse diameter of the spinal cord with a rigid flat plate, the stress on the spinal cord was very low at 10% compression of the AP diameter of the spinal cord. At 20% compression, the stress increased in the gray matter and anterior funiculi of both sides. At 30% compression, the stress on the spinal cord was increased and high levels of stress were observed in the gray matter of both sides, as well as in the anterior, lateral and posterior funiculi of both sides (Fig. 3E).

Discussion

BSS was first described by Brown-Séquard in a study of a patient who was suffering from a knife injury and who presented with hemicord syndrome (9). BSS involves ipsilateral loss of motor function resulting from corticospinal tract interruption, combined with a contralateral loss of pain and temperature sensation as a result of spinothalamic tract dysfunction. BSS is most often observed in association with traumatic injuries to the spinal cord (10-12). The incidence of complete BSS due to chronic compression is very low. In one study, complete BSS was observed in 4.6% of 600 cases reported as BSS (4) and these comprised trauma (1.0%), tumoral compression (0.8%) and non-tumoral compression or non-compressive lesions (2.8%). The contribution of cervical disc herniation to BSS has been estimated by Jomin *et al* (13) to be 2.6%, but no further details were provided in this study. Choi *et al* (14) reported that only five of the 2,350 cases (0.21%) in their series were retrospectively evaluated as complete BSS caused by cervical disc herniation. Nine percent of the patients who presented with symptoms of thoracic disc herniation were diagnosed with BSS (15), but this study did not classify cases into complete or incomplete BSS. BSS may also constitute the initial symptom for idiopathic spinal cord herniation (ISCH), a rare cause of progressive myelopathy (16-19). ISCH is characterized by spontaneous herniation of the spinal cord through an anterior or antero-lateral dural defect. A review of the literature relevant to ISCH showed that 73/100 reported cases (73%) presented with BSS, 19 (19%) with spasticity and eight (8%) with numbness or leg pain (20) However, this study did not provide details concerning whether the BSS was complete or incomplete.

Based on these previous findings, we hypothesized that pressure within a limited range of compression causes complete BSS with static compression. To test this hypothesis, we investigated three different degrees of static compression under five different compressions of the transverse diameter of the spinal cord. We calculated the stress distributions inside the spinal cord and simulated complete and incomplete BSS using a 3D-FEM model.

The aim of the present study was to develop a 3D-FEM spinal cord model that simulates the clinical situation. In a similar manner to previous studies by Kato *et al* (21-23), Li *et al* (24,25) and Nishida *et al* (26,27), bovine spinal cord or magnetic resonance imaging (MRI) was used in the model for the present analysis since it was not possible to obtain fresh human spinal cord. The mechanical properties of the spinal cord used in the present study were similar to those reported in earlier studies (6-8). Li and Dai (24) noted that it was reasonable to make use of the mechanical properties of bovine spinal cord since the brains and spinal cords of cattle and humans exhibit similar changes when injured. In the present study, we also assumed that the mechanical properties of the spinal cords from the two species were similar. Persson *et al* (5) described the division of spinal cord into pia mater and white and gray matter, and demonstrated that the presence of pia mater had a significant effect on spinal cord deformation; thus, pia mater is required to simulate the clinical situation effectively.

The present study was limited to the investigation of stress distribution caused by compression. Additional casual factors that may contribute to cervical spondylotic myelopathy (CSM) include ischemia, congestion and spinal cord stretch injury (28). Blood flow was not analyzed in this FEM analysis and only one movement (static compression) was investigated for potential association with BSS. Long-term compression and apoptotic factors were not considered in this FEM analysis. Moreover, the FEM model used in the present study was simplified in order to facilitate the calculations. Analysis errors were reduced by using a FEM mesh, assuming the spinal cord was symmetric, not including the denticulate ligament, dura and nerve root sheaths, and setting a close distance between the spinal cord and lamina, spinal cord and anterior compression of the spinal cord.

When the rigid-flat-plate compression was applied to <37.5% of the length of the transverse diameter of spinal cord, the stress on the gray matter, anterior funiculus and lateral funiculus was increased, but not the stress on the posterior funiculus. Consequently, contralateral loss of pain, temperature sensation and ipsilateral loss of motor function are likely to occur, but not ipsilateral disorders of vibration and position sense. This may correspond to cases of incomplete BSS.

When the rigid-flat-plate compression was applied to >62.5% of the length of the transverse diameter of the spinal cord, the stress increased on the gray matter, the anterior funiculi and the posterior funiculi on both sides and on the lateral funiculus on the compression side, but not the lateral funiculus on the non-compression side. Based on these results, the loss of pain and temperature sensation, as well as ipsilateral loss of motor function on the compression side are expected to occur. Disorders of vibration and position sense are also likely

to occur and, thus, this situation may correspond to cases with incomplete BSS.

Under a rigid-flat-plate compression of 50% of the length of the transverse diameter of the spinal cord and compression of 10% of the AP diameter of the spinal cord, the stress levels in the gray matter were very low. At 20% compression, the stress levels were slightly increased in the gray matter and anterior funiculus, while at 30% compression, the levels of stress were increased in the gray matter, as well as in the anterior, lateral and posterior funiculi. This may result in the contralateral loss of pain and temperature sensation due to anterior funiculus compression, ipsilateral loss of motor function due to lateral funiculus compression, and ipsilateral disorders of vibration and position sense due to posterior funiculus compression. However, the distribution of stress to the posterior funiculus of the non-compressed side and was not observed; thus, this may correspond to cases of complete BSS.

The simulation model used in the present study showed that only at a compression of 50% of the length of the transverse diameter of the spinal cord did the stress distribution lead to complete BSS. However, compression within such a limited range is an infrequent clinical event and, thus, this may explain why the number of cases of complete BSS associated with chronic compression is rare.

References

1. Kraus JA, Stuper BK and Berlit P: Multiple sclerosis presenting with Brown-Séquard syndrome. J Neurol Sci 156: 112-113, 1998.
2. Fisher RG: Protrusions of thoracic disc. The factor of herniation through the dura matter. J Neurosurg 22: 591-593, 1965.
3. Love JG and Schorn VG: Thoracic-disc protrusions. JAMA 191: 627-631, 1965.
4. Koehler PJ and Endtz LJ: The Brown-Séquard syndrome. True or false? Arch Neurol 43: 921-924, 1986.
5. Persson C, Summers J and Hall RM: The importance of fluid-structure interaction in spinal trauma models. J Neurotrauma 28: 113-125, 2011.
6. Ichihara K, Taguchi T, Shimada Y, Sakuramoto I, Kawano S and Kawai S: Gray matter of the bovine cervical spinal cord is mechanically more rigid and fragile than the white matter. J Neurotrauma 18: 361-367, 2001.
7. Ichihara K, Taguchi T, Sakuramoto I, Kawano S and Kawai S: Mechanism of the spinal cord injury and the cervical spondylotic myelopathy: new approach based on the mechanical features of the spinal cord white and gray matter. J Neurosurg 99 (Suppl 3): 278-285, 2003.
8. Tunturi AR: Elasticity of the spinal cord, pia, and denticulate ligament in the dog. J Neurosurg 48: 975-979, 1978.
9. Brown Sequard CE: De la transmission des impressions sensitives par la moelle epiniere. CR Soc Biol 1: 192-194, 1849.
10. Kobayashi N, Asamoto S, Doi H and Sugiyama H: Brown-Séquard syndrome produced by cervical disc herniation: report of two cases and review of the literature. Spine J 23: 530-533, 2003.
11. Kohno M, Takahashi H, Yamakawa K, Ide K and Segawa H: Postoperative prognosis of Brown-Séquard-type myelopathy in patients with cervical lesions. Surg Neurol 51: 241-246, 1999.
12. Mastronardi and Ruggeri A: Cervical disc herniation producing Brown-Séquard syndrome: case report. Spine (Phila Pa 1976) 29: E28-E31, 2004.
13. Jomin M, Lesoin F, Lozes G, *et al*: Herniated cervical discs. Analysis of a series of 230 cases. Acta Neurochir (Wien) 79: 107-113, 1986.
14. Choi KB, Lee CD, Chung DJ and Lee SH: Cervical disc herniation as a cause of Brown-Séquard syndrome. J Korean Neurosurg Soc 46: 505-510, 2009.
15. Arce CA and Dohrmann GJ: Herniated thoracic disks. Neurol Clin 3: 383-392, 1985.
16. Massicotte EM, Montanera WR, Ross Fleming JF, Tucker WS, Willinsky R, TerBrugge K and Fehlings MG: Idiopathic spinal cord herniation: report of eight cases and review of the literature. Spine (Phila Pa 1976) 27: E233-E241, 2002.
17. Miyaguchi M, Nakamura H, Shakudo M, Inoue Y and Yamano Y: Idiopathic spinal cord herniation associated with intervertebral disc extrusion: a case report and review of the literature. Spine (Phila Pa 1976) 26: 1090-1094, 2001.
18. Wada E, Yonebu K and Kang J: Idiopathic spinal cord herniation: report of three cases and review of the literature. Spine (Phila Pa 1976) 25: 1984-1988, 2000.
19. White BD and Tsegaye M: Idiopathic anterior spinal cord hernia: under-recognized cause of thoracic myelopathy. Br J Neurosurg 18: 246-249, 2004.
20. Sasari M, Ozer AF, Vural M and Sarioglu AC: Idiopathic spinal cord herniation: case report and review of the literature. J Spinal Cord Med 32: 86-94, 2009.
21. Kato Y, Kataoka H, Ichihara K, *et al*: Biomechanical study of cervical flexion myelopathy using a three-dimensional finite element method. J Neurosurg Spine 8: 436-441, 2008.
22. Kato Y, Kanchiku T, Imajo Y, *et al*: Flexion model simulating spinal cord injury without radiographic abnormality in patients with ossification of the longitudinal ligament: the influence of flexion speed on the cervical spine. J Spinal Cord Med 32: 555-559, 2009.
23. Kato Y, Kanchiku T, Imajo Y, *et al*: Biomechanical study of the effect of the degree of static compression of the spinal cord in ossification of the posterior longitudinal ligament. J Neurosurg Spine 12: 301-305, 2010.
24. Li XF and Dai LY: Three-dimensional finite element model of the cervical spinal cord: preliminary results of injury mechanism analysis. Spine (Phila Pa 1976) 34: 1140-1147, 2009.
25. Li XF and Dai LY: Acute central cord syndrome: injury mechanisms and stress features. Spine (Phila Pa 1976) 35: E955-E964, 2010.
26. Nishida N, Kato Y, Imajo Y, Kawano S and Taguchi T: Biomechanical study of the spinal cord in thoracic ossification of the posterior longitudinal ligament. J Spinal Cord Med 34: 518-522, 2011.
27. Nishida N, Kato Y, Imajo Y, Kawano S and Taguchi T: Biomechanical analysis of cervical spondylotic myelopathy: the influence of dynamic factors and morphometry of the spinal cord. J Spinal Cord Med 35: 256-261, 2012.
28. Henderson FC, Geddes JF, Vaccaro AR, Woodard E, Berry KJ and Benzel EC: Stretch-associated injury in cervical spondylotic myelopathy: new concept and review. Neurosurgery 56: 1101-1113, 2005.

Anti-interleukin-6 receptor antibody reduces neuropathic pain following spinal cord injury in mice

TOMOTOSHI MURAKAMI[1], TSUKASA KANCHIKU[1], HIDENORI SUZUKI[1], YASUAKI IMAJO[1], YUICHIRO YOSHIDA[1], HIROSHI NOMURA[2], DAN CUI[3], TOSHIZO ISHIKAWA[4], EIJI IKEDA[3] and TOSHIHIKO TAGUCHI[1]

[1]Department of Orthopedic Surgery, Yamaguchi University Graduate School of Medicine, Ube, Yamaguchi 755-8505; [2]Department of Orthopedic Surgery, Hiroshima Red Cross Hospital, Hiroshima, Hiroshima 730-0052; Departments of [3]Pathology and [4]Neurosciences, Yamaguchi University Graduate School of Medicine, Ube, Yamaguchi 755-8505, Japan

Received April 27, 2013; Accepted August 29, 2013

DOI: 10.3892/etm.2013.1296

Abstract. The present study reports the beneficial effects of an anti-mouse interleukin-6 (IL-6) receptor antibody (MR16-1) on neuropathic pain in mice with spinal cord injury (SCI). Following laminectomy, contusion SCI models were produced using an Infinite Horizon (IH)-impactor. MR16-1 was continuously injected for 14 days using Alzet osmotic pumps. A mouse IL-6 ELISA kit was then used to analyze IL-6 levels in the spinal cord tissue between 12 and 72 h after injury. Motor and sensory functions were evaluated each week using the Basso Mouse Scale (BMS), plantar von Frey and thermal threshold tests. Histological examinations were performed 42 days after SCI. Between 24 and 72 h after SCI, the expression levels of IL-6 were significantly decreased in the MR16-1 treated group. Six weeks after surgery, the BMS score of the MR16-1-treated group indicated significant recovery of neurological functions. MR16-1-treated mice in the SCI group exhibited lower paw withdrawal thresholds in the plantar von Frey and thermal tests, which were used to evaluate allodynia. MR16-1 treatment significantly increased the area of Luxol fast blue-stained tissue, representing spared myelin sheaths. These results indicate that the continuous inhibition of IL-6 signaling by MR16-1 between the early and sub-acute phases following SCI leads to neurological recovery and the suppression of hyperalgesia and allodynia. Overall, our data suggest that the inhibition of severe inflammation may be a promising neuroprotective approach to limit secondary injury following SCI and that an anti-IL-6 receptor antibody may have clinical potential for the treatment of SCI.

Correspondence to: Dr Tomotoshi Murakami, Department of Orthopedic Surgery, Yamaguchi University Graduate School of Medicine, 1-1-1 Minamikogushi, Ube, Yamaguchi 755-8505, Japan
E-mail: t-murakami@ogoridaiichi.jp

Key words: spinal cord injury, inflammation, interleukin-6, hyperalgesia, allodynia

Introduction

Over two-thirds of individuals with spinal cord injury (SCI) experience the effects of neuropathic pain in their daily lives. Neuropathic pain is resistant to general analgesic treatment and is a long-term issue for SCI patients. SCI causes severe motor and sensory dysfunction, while neuroinflammation is an important secondary event in the injury cascade. The development of strategies to minimize this auto-destructive injury is one of the main aims in the field of SCI research. A number of studies have demonstrated remarkable protection and functional recovery using anti-inflammatory reagents in SCI models (1-7). However, to date, there have been no studies concerning the use of anti-inflammatory reagents to reduce neuropathic pain following SCI. The interleukin-6 (IL-6) cytokine is important in mediating pro-inflammatory damage after SCI (8-10). Activation of the Janus kinase and signal transducer and activator of transcription 3 (JAK-STAT3) signaling pathway by IL-6 is an important mechanism for transducing signals from the cell surface and is strongly linked to immune/inflammatory reactions (11,12). Early activation of this pathway occurs most often in spinal microglia and contributes to the development of neuropathic pain (13-15). Attenuation of IL-6 activity is therefore an attractive therapeutic strategy for reducing the neurological deficits associated with SCI. The present study reports a significant reduction of neuropathic pain in mice with SCI following the administration of anti-mouse IL-6 receptor antibody (MR16-1).

Materials and methods

Experimental procedures. All experiments were approved by the Ethics Committee for Animal Studies at Yamaguchi University (Ube, Japan) and were carried out in accordance with the Guidelines for Proper Conduct of Animal Experiments, Science Council of Japan (June 1, 2006).

MR16-1. The rat anti-mouse IL-6 receptor monoclonal antibody (MR16-1), a gift from Chugai Pharmaceuticals Co. Ltd., (Tokyo, Japan), was prepared as described previously (16).

An isotype of this antibody is IgG1. MR16-1 has been shown to bind to the soluble mouse IL-6 receptor and suppress IL-6-induced cellular responses in a dose-dependent manner. Other basic characterizations of this antibody have been described in previously published reports (8).

Animals and surgery. Sixty adult female C57BL/6J mice (10 weeks old) were obtained from Japan SLC, Inc. (Shizuoka, Japan) and assigned to the following groups: The MR16-1 group, comprising MR16-1-treated mice (n=25); the control group, comprising untreated SCI mice (n=25); and the sham group, comprising mice subjected to laminectomy but with normal spinal cords (n=10). Mice were anesthetized with an intraperitoneal injection of ketamine (100 mg/kg) and xylazine (10 mg/kg). Laminectomy was performed at the level of the 10th thoracic vertebra under a surgical microscope. A contusion SCI model was produced using an Infinite Horizon (IH)-impactor (PSI Inc., Lexington, KY, USA) with an impact force of 60 kdyn (17). Immediately after injury, MR16-1 was continuously injected for 1-14 days (150μg/day) using Alzet osmotic pumps (DURECT Corporation., Cupertino, CA, USA).

ELISA analysis of interleukin-6 concentration. Spinal cord tissue (5 mm in length) at the lesion epicenter was dissected in each group (5 animals per group) at 12, 24 and 72 h after injury. Spinal cord tissue samples to be used for ELISA analysis were homogenized in radio-immunoprecipitation assay (RIPA) lysis buffer (500 μl; Santa Cruz Biotechnology, Inc., Santa Cruz, CA, USA) and the IL-6 concentration was measured using a mouse IL-6 ELISA kit (Invitrogen Life Technologies, Carlsbad, CA, USA) according to the manufacturer's instructions. The IL-6 levels were expressed in pg/mg (18).

Assessment of motor function recovery. The Basso Mouse Scale (BMS) is a validated scale used to monitor the progress of hind-limb functional recovery following SCI. The scale ranges from 0 (no ankle movement) to 9 (complete functional recovery) points (19). BMS scores were recorded at 3, 7, 14, 21, 28 and 42 days following SCI by two independent examiners who were blind to the experimental conditions. Hind-limb motion was used to assess coordinated movement and stepping. When differences in the BMS score between the right and left hind limbs were observed, the average of the two scores was used.

Assessment of sensory function recovery and allodynia. Sensory tests were performed 21 and 42 days after SCI. All behavioral tests were conducted by an experienced investigator who was blind to the type of intervention. Each hind paw was tested three times. Paw withdrawal latencies to heat were measured according to the Hargreaves' method (20) by applying a standard Plantar test (Ugo Basile, Comerio, Italy). The animals were placed on a glass surface and a radiant heat source was positioned under one hind paw. The latency to paw withdrawal was recorded automatically. Paw withdrawal thresholds to tactile stimulation were measured according to the von Frey test using a standard Dynamic Plantar Aesthesiometer (Ugo Basile). The animals were placed in plexiglass cages on a wire mesh. The plantar surface of the hind paw was probed with a von Frey monofilament (21) and the force required for paw withdrawal was recorded automatically. The von Frey filament and thermal threshold tests were used to measure mechanical allodynia and thermal hyperalgesia, respectively.

Histological analysis. Spinal cords were harvested 42 days after surgery. Mice were anesthetized with an intraperitoneal injection of ketamine (100 mg/kg) and xylazine (10 mg/kg) and then perfused with 4% paraformaldehyde. A 1-cm length of spinal cord that included the lesion center was removed and frozen for sectioning. The tissue was sectioned axially in 10-μm-thick sections. Transverse sections from the injury epicenter were also stained for myelin using Luxol fast blue (LFB). LFB-positive areas in which the density significantly exceeded the threshold of each background were calculated as the percentage cross-sectional area of residual tissue. Tissue sections were analyzed using the Cavalieri Probe (Stereo Investigator 64-bit software; MBF Bioscience, Williston, VT, USA) (22).

Electrophysiological evaluation. Sensory evoked potentials (SEPs) were recorded from the MR16-1 (n=10), control (n=10) and sham (n=5) groups 42 days after SCI. SEPs following sciatic nerve electrical train stimulation were recorded from the sensory cortex of the brain in mice anesthetized with ketamine. A ground electrode was inserted subcutaneously between the stimulating and recording electrodes and a constant current stimulus (S) of 0.1 msec duration and 2.0 mA intensity was applied at a rate of 5.7 Hz to the hind paw. At a band-width of 10-3,000 Hz, a total of 200 traces were averaged and replicated (23). SEP peak latency and amplitude were measured from the start of S to the peak of the first positive peak (P1).

Statistical analysis. All data in this study are expressed as the mean ± SEM. ELISA data and electrophysiological latency data were analyzed using a one-way ANOVA. The BMS and histological data were analyzed using a two-way ANOVA for repeated measures. Significant ANOVA results were followed by post-hoc Bonferroni analysis. Sensory variables showed normal distribution in the Kolmogorow-Smirnow test. $P<0.05$ was considered to indicate a statistically significant difference.

Results

ELISA data. At 12 h after SCI, the expression levels of IL-6 were 430.6±66.8, 362.1±42.3 and 80.0±12.0 pg/mg in the MR16-1, control and sham groups, respectively. No significant differences in the expression levels of IL-6 in the spinal cord were identified between the MR16-1 and control groups 12 h after SCI. At 24-72 h after SCI, the expression of IL-6 in injured spinal cord tissue was significantly lower in the MR16-1 group than in the control group (Fig. 1).

At 24 h following SCI, the expression levels of IL-6 were 258.0±44.7, 503.3±24.0 and 78.0±12.0 pg/mg in the MR16-1, control and sham groups, respectively. At 72 h after SCI, the expression levels of IL-6 were 111.2±6.9, 166.4±5.0 and 77.0±11.5 pg/mg in the MR16-1, control and sham groups, respectively. Between 72 h and 2 weeks following SCI, no

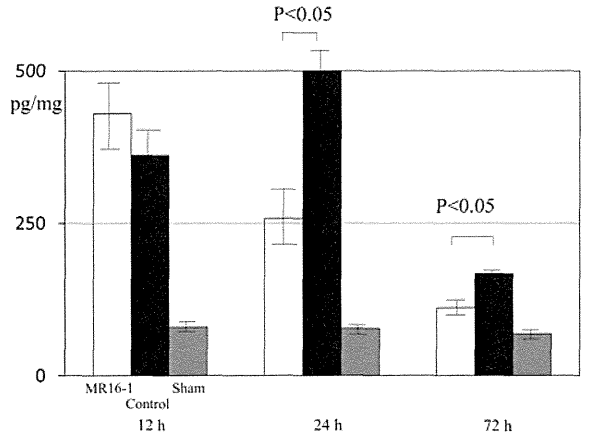

Figure 1. ELISA data. Time course for the expression of IL-6 in spinal cord tissue following SCI. The graph shows IL-6 expression in the normal spinal cords of mice from the sham group. No significant differences in the expression of IL-6 were identified between the MR16-1 and control groups 12 h after SCI. Between 24 and 72 h after SCI, the expression of IL-6 in injured spinal cord tissue was significantly lower in the MR16-1 group than in the control group. SCI, spinal cord injury; IL-6, interleukin-6; MR16-1, anti-mouse IL-6 receptor antibody.

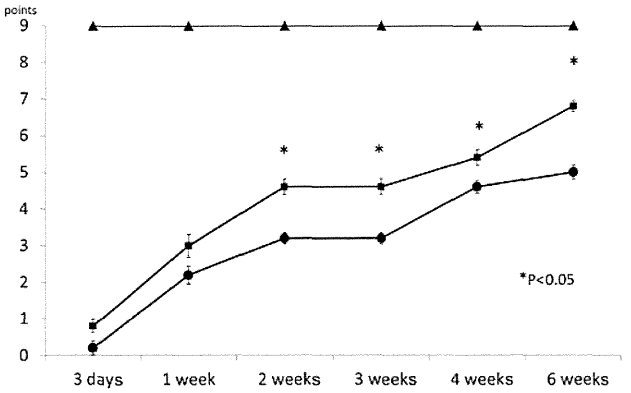

Figure 2. Time course of BMS score following SCI. Between 2 and 6 weeks after SCI, the MR16-1 group exhibited significantly improved recovery compared with the control group. BMS, Basso Mouse Scale; SCI, spinal cord injury; MR16-1. anti-mouse interleukin-6 receptor antibody; ■, BMS scores for the MR16-1 group; ●, BMS scores for the control group; ▲, BMS scores for the sham group. *P<0.05, MR16-1 group vs. control group.

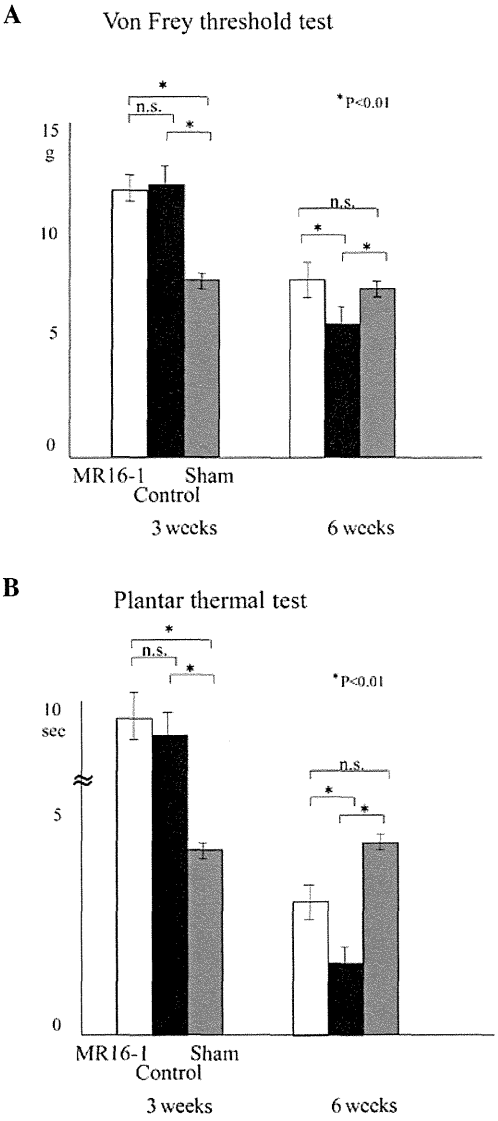

Figure 3. Results of (A) von Frey threshold and (B) plantar thermal tests of sensory functions and allodynia. Three weeks after SCI, the majority of mice were under hypesthesia, thus allodynia could not be evaluated. Six weeks after SCI, hyperalgesia was significantly suppressed in MR16-1 group mice compared with the control group. The data for control group represent the natural course for sensory recovery in SCI mice following a 60-kdyn impact, while the data for the sham group represent normal sensory function without neurological deficit. SCI, spinal cord injury; MR16-1. anti-mouse interleukin-6 receptor antibody; n.s., not significant.

significant differences were identified in the expression levels of IL-6 in the spinal cord among the three groups.

Motor function. Mice injected with MR16-1 showed continuous recovery of motor function. Three days after surgery, the BMS score was 0.8±0.18 for the MR16-1 group, 0.2±0.18 for the control group and 9.0±0.00 for the sham group (Fig. 2). One week after surgery, the BMS score was 3.0±0.31 for the MR16-1 group, 2.2±0.24 for the control group and 9.0±0.00 for the sham group. Two weeks after surgery, the BMS score was 4.6±0.22 for the MR16-1 group, 3.2±0.16 for the control group and 9.0±0.00 for the sham group. Three weeks after surgery, the BMS score was 4.6±0.22 for the MR16-1 group, 3.2±0.16 for the control group and 9.0±0.00 for the sham group. Four weeks after surgery, the BMS score was 5.4±0.22 for the MR16-1 group, 4.6±0.17 for the control group and 9.0±0.00 for the sham group. Six weeks after surgery, the BMS score was 6.8±0.15 for the MR16-1 group, 5.0±0.19 for the control group and 9.0±0.00 for the sham group. Between 2 and 6 week after SCI, the BMS scores between the MR16-1 and sham groups were significantly different.

The BMS scores for the MR16-1 and control groups indicated gradual recovery one week after SCI. However, between 2 and 6 weeks following MR16-1 treatment, mice in the MR16-1 group showed a marked recovery compared with those in the control group (Fig. 2).

Sensory functional recovery and prevention of allodynia. The mice that were continuously infused with MR16-1 showed recovery of sensory function (Fig. 3). The sensory scores of the mice in the von Frey and thermal tests were as

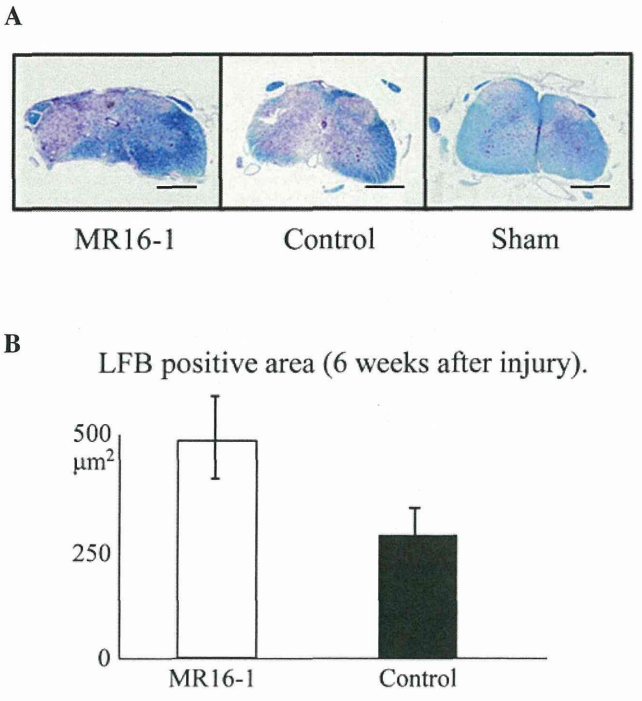

Figure 4. (A) LFB-stained spinal cord at the center of the SCI (scale bar, 50 μm). The LFB-positive area was significantly greater in the MR16-1 group. (B) The area of preserved myelin sheath was significantly higher in the MR16-1 group than in the control group. SCI, spinal cord injury; LFB, luxol fast blue; MR16-1, anti-mouse interleukin-6 receptor antibody.

follows: in the MR16-1 group 3 weeks after SCI, 11.7±0.64 g and 9.8±0.86 sec, respectively, and at 6 weeks, 7.0±0.84 g and 2.9±0.37 sec, respectively; in the control group 3 weeks after SCI, 11.9±0.69 g and 9.2±0.82 sec, respectively and at 6 weeks, 5.3±1.1 g and 1.7±0.27 sec, respectively; in the sham group 3 weeks after SCI, 6.9±0.26 g and 4.2±0.23 sec, respectively, and at 6 weeks, 6.4±0.24 g and 4.5±0.21 sec, respectively.

At 3 weeks after SCI, the majority of mice were in the recovery phase for sensory function. It was not possible to evaluate the occurrence of allodynia since the majority of mice were under hypesthesia. Six weeks after SCI, hyperalgesia was significantly suppressed in the MR16-1 group compared with the control group. The data for the control group demonstrate the natural course of sensory recovery in SCI, while the data for the sham group demonstrate normal sensory evaluation without neurological deficit.

LFB stain. The area of Luxol fast blue-stained tissue, representing spared myelin sheath, was significantly increased as a result of treatment with MR16-1 (Fig. 4A).

The LFB-positive area at the center of the axial section of the SCI was 482±22 μm^2 in the MR16-1 group and 263±43 μm^2 in the control group (Fig. 4B), demonstrating significant preservation in the MR16-1 group.

SEPs. SEP recordings were performed 6 weeks after SCI in order to provide electrophysiological evidence for the recovery of sensory function. The latency of the first wave was 7.4±1.1 msec in the MR16-1 group, 7.7±0.9 msec in the control group and 7.1±0.5 msec in the sham group (no significant differences were identified). However, the amplitude of the first wave was 9.1±1.9 msec in the MR16-1 group, 4.6±0.8 msec in the control group and 14.1±0.7 msec in the sham group. The amplitude for the MR16-1 group was significantly lower than that of the sham group, but significantly higher than that of the control group. MR16-1-treated SCI mice exhibited suppressed allodynia and increased sensory function, as determined by electrophysiological measurements.

Discussion

Chronic pain and allodynia following SCI represent a therapeutic challenge. To the best of our knowledge, the present study is the first report demonstrating that MR16-1 suppresses allodynia and hyperalgesia in mice with SCI. Mice treated with MR16-1 exhibited only moderate hyperalgesia of the lower limbs.

A previous study reported that the administration of IL-6 cytokine at lesion sites one day after injury increased the recruitment and the peak of macrophage, neutrophil and microglial cell activity at the lesion sites to a greater extent than when administered 4 days after injury (24). In the present study, the concentration of IL-6 at the injury site between 24 and 72 h after SCI was significantly reduced in mice treated with MR16-1. These mice also exhibited improved locomotor BMS scores from 14 days after SCI compared with untreated mice. This result suggests that MR16-1 conferred a neuroprotective effect in SCI mice. This is in agreement with a previous study in which MR16-1 treatment for SCI decreased connective tissue formation due to astrogliosis (25). The suppression of gliosis leads to protection of the myelin sheath in the injured spinal cord (25). In the present study, an increase in myelin preservation was also observed, as revealed by LFB staining at 42 days post-injury. Furthermore, SEPs confirmed that MR16-1 treatment for SCI led to electrophysiological sensory recovery. In this study, cord dysfunction at the thoracic level was revealed by recording hind-limb SEPs following SCI. Potentials evoked in hind-limbs appeared as well-characterized peaks, and provide a sensitive and quantitative measure to detect pathological changes following SCI. This is in accordance with a number of clinical studies reporting that pathological changes in SEPs are a sensitive method for the detection of the extent of cord injury (23). Although this method primarily represents the function of the somatosensory pathways, SEPs have been used extensively in neurophysiological assessments of spinal cord integrity (23,26).

IL-6 is one of the major proinflammatory cytokines that triggers secondary injury in the pathophysiology of SCI. It is known to promote the activation and infiltration of macrophages and microglia, the major inflammatory cells observed in SCI (9). When IL-6 is released, it binds to the membrane-bound IL-6 receptor (IL-6R) to form an IL-6/IL-6R complex that associates with the signal transducer, gp130, transmitting a signal into cells (16). In addition, the gp130-JAK/STAT pathway promotes the differentiation of astrocytes. These cells produce a chondroitin sulfate proteoglycan (CSPG) that forms a glial scar. Therefore, the overexpression of IL-6 enhances inflammation and tissue injury (25). By contrast, previous studies using gene-knockout animals have revealed that the excessive inhibition of IL-6

signaling is detrimental to functional recovery, since it inhibits axonal regeneration or causes failed gliosis, which implies that IL-6 may also have a beneficial function in spinal cord repair (9,25). Based on these findings and the theory that a blockade of IL-6 signaling may reduce the extent of post-SCI inflammatory damage, previous researchers have administered MR16-1 following SCI and demonstrated reduced inflammation, decreased astrogliosis and enhanced tissue sparing, leading to improved functional recovery.

In conclusion, the present results suggest that continuous blockade of IL-6 signaling following SCI reduces damaging inflammatory activity, thus promoting functional and sensory recovery. A humanized antibody against human IL-6 receptor (MRA; tocilizumab) is already in clinical use for the treatment of rheumatoid arthritis. This drug may also represent a novel option for the treatment of human SCI.

References

1. Donnelly DJ and Popovich PG: Inflammation and its role in neuroprotection, axonal regeneration and functional recovery after spinal cord injury. Exp Neurol 209: 378-388, 2008.
2. Jones TB, McDaniel EE and Popovich PG: Inflammatory-mediated injury and repair in the traumatically injured spinal cord. Curr Pharm Des 11: 1223-1236, 2005.
3. Popovich PG and Jones TB: Manipulating neuroinflammatory reactions in the injured spinal cord: back to basics. Trends Pharmacol Sci 24: 13-17, 2003.
4. Schwab JM, Brechtel K, Mueller CA, *et al*: Experimental strategies to promote spinal cord regeneration - an integrative perspective. Prog Neurobiol 78: 91-116, 2006.
5. Thuret S, Moon LD and Gage FH: Therapeutic interventions after spinal cord injury. Nat Rev Neurosci 7: 628-643, 2006.
6. Lee HL, Lee KM, Son SJ, Hwang SH and Cho HJ: Temporal expression of cytokines and their receptors mRNAs in a neuropathic pain model. Neuroreport 15: 2807-2811, 2004.
7. Siddall P, Xu CL and Cousins M: Allodynia following traumatic spinal cord injury in the rat. Neuroreport 6: 1241-1244, 1995.
8. Okada S, Nakamura M, Mikami Y, *et al*: Blockade of interleukin-6 receptor suppresses reactive astrogliosis and ameliorates functional recovery in experimental spinal cord injury. J Neurosci Res 76: 265-276, 2004.
9. Mukaino M, Nakamura M, Yamada O, *et al*: Anti-IL-6-receptor antibody promotes repair of spinal cord injury by inducing microglia-dominant inflammation. Exp Neurol 224: 403-414, 2010.
10. Lacroix S, Chang L, Rose-John S and Tuszynski MH: Delivery of hyper-interleukin-6 to the injured spinal cord increases neutrophil and macrophage infiltration and inhibits axonal growth. J Comp Neurol 454: 213-228, 2002.
11. Hirano T, Nakajima K and Hibi M: Signaling mechanisms through gp130: a model of the cytokine system. Cytokine Growth Factor Rev 8: 241-252, 1997.
12. Cattaneo E, Conti L and De-Fraja C: Signalling through the JAK-STAT pathway in the developing brain. Trends Neurosci 22: 365-369, 1999.
13. Dominguez E, Rivat C, Pommier B, Mauborgne A and Pohl M: JAK/STAT3 pathway is activated in spinal cord microglia after peripheral nerve injury and contributes to neuropathic pain development in rat. J Neurochem 107: 50-60, 2008.
14. Yamauchi K, Osuka K, Takayasu M, *et al*: Activation of JAK/STAT signalling in neurons following spinal cord injury in mice. J Neurochem 96: 1060-1070, 2006.
15. Dominguez E, Mauborgne A, Mallet J, Desclaux M and Pohl M: SOCS3-mediated blockade of JAK/STAT3 signaling pathway reveals its major contribution to spinal cord neuroinflammation and mechanical allodynia after peripheral nerve injury. J Neurosci 30: 5754-5766, 2010.
16. Okazaki M, Yamada Y, Nishimoto N, Yoshizaki K and Mihara M: Characterization of anti-mouse interleukin-6 receptor antibody. Immunol Lett 84: 231-240, 2002.
17. Scheff SW, Rabchevsky AG, Fugaccia I, Main JA and Lumpp JE Jr: Experimental modeling of spinal cord injury: characterization of a force-defined injury device. J Neurotrauma 20: 179-193, 2003.
18. Nakajima Y, Osuka K, Seki Y, *et al*: Taurine reduces inflammatory responses after spinal cord injury. J Neurotrauma 27: 403-410, 2010.
19. Basso DM, Fisher LC, Anderson AJ, Jakeman LB, McTigue DM and Popovich PG: Basso Mouse Scale for locomotion detects differences in recovery after spinal cord injury in five common mouse strains. J Neurotrauma 23: 635-659, 2006.
20. Hargreaves K, Dubner R, Brown F, Flores C and Joris J: A new and sensitive method for measuring thermal nociception in cutaneous hyperalgesia. Pain 32: 77-88, 1988.
21. Kim HY, Wang J, Lu Y, Chung JM and Chung K: Superoxide signaling in pain is independent of nitric oxide signaling. Neuroreport 20: 1424-1428, 2009.
22. Chen KB, Uchida K, Nakajima H, *et al*: Tumor necrosis factor-α antagonist reduces apoptosis of neurons and oligodendroglia in rat spinal cord injury. Spine (Phila Pa 1976) 36: 1350-1358, 2011.
23. Cho N, Nguyen DH, Satkunendrarajah K, Branch DR and Fehlings MG: Evaluating the role of IL-11, a novel cytokine in the IL-6 family, in a mouse model of spinal cord injury. J Neuroinflammation 9: 134, 2012.
24. Klusman I and Schwab ME: Effects of pro-inflammatory cytokines in experimental spinal cord injury. Brain Res 762: 173-184, 1997.
25. Guerrero AR, Uchida K, Nakajima H, *et al*: Blockade of interleukin-6 signaling inhibits the classic pathway and promotes an alternative pathway of macrophage activation after spinal cord injury in mice. J Neuroinflammation 9: 40, 2012.
26. Chandran AP, Oda K, Shibasaki H and Pisharodi M: Spinal somatosensory evoked potentials in mice and their developmental changes. Brain Dev 16: 44-51, 1994.

ACRM
AMERICAN CONGRESS OF REHABILITATION MEDICINE

Archives of Physical Medicine and Rehabilitation

journal homepage: www.archives-pmr.org

Archives of Physical Medicine and Rehabilitation 2013;94:467-73

ORIGINAL ARTICLE

T-Reflex Studies in Human Upper Limb Muscles During Voluntary Contraction: Normative Data and Diagnostic Value for Cervical Radiculopathy

Tomoko Tetsunaga, MD,[a,b] Toshikazu Tani, MD,[a] Masahiko Ikeuchi, MD,[a] Kenji Ishida, MD,[c] Kazunobu Kida, MD,[a] Nobuaki Tadokoro, MD,[a] Masahiro Ichimiya, PhD,[d] Noriaki Nakajima, PhD,[e] Hideshi Tsuboya, MD,[f] Shinichirou Taniguchi, MD[g]

From the Departments of [a]Orthopaedic Surgery and [c]Physical Medicine and Rehabilitation, and the [e]Center of Medical Information Science, Kochi Medical School, Kohasu Oko-cho, Nankoku; [b]Department of Orthopaedic Surgery, Okayama University Hospital, Kitaku, Okayama; [d]Department of Electrical and Electronic Engineering, Tokushima University Faculty of Engineering, Tokushima; [f]Department of Orthopaedic Surgery, Shimanto City Hospital, Shimanto; and [g]Department of Orthopaedic Surgery, Kansai Medical University Takii Hospital, Osaka, Japan.

Abstract

Objective: To evaluate the diagnostic utility of the T reflexes elicited from the upper limb muscles during standardized volitional contraction monitored by a real-time integrating electromyographic analyzer.

Design: Prospective descriptive study.

Setting: Department of orthopedic surgery at a university hospital.

Participants: Healthy subjects (n=80) evenly distributed across decades of age from 21 to 79 years, and 12 consecutive patients with a single cervical root lesion based on clinical and magnetic resonance imaging studies and diagnostic block.

Interventions: Not applicable.

Main Outcome Measures: Using a special hammer, which externally triggers the sweep on skin contact, we evoked T reflexes in the biceps (C5), brachioradialis (C6), triceps (C7), and the first dorsal interosseous muscles (C8).

Results: Simultaneous regression analyses yielded clinically useful upper limits of normative values for latencies, side-to-side differences, and amplitude ratios adjusted to age and arm span. Comparison of the T reflexes between the 2 sides localized the solitary root lesions with a high sensitivity (92%), specificity (81%), and accuracy (83%). T-reflex studies proved helpful to localize the lesion even in patients who solely complained of upper limb pain.

Conclusions: The T reflexes with a standardized facilitation of the upper limb muscles provide a clinically useful, noninvasive measure to localize the C5 to C8 radiculopathies. This study contributes in reassessing the currently underused T reflex as an electrodiagnostic technique.

Archives of Physical Medicine and Rehabilitation 2013;94:467-73

In cervical radiculopathy (CR), the distribution of motor deficits provides more reliable localization than sensory impairments, which show dermatomal overlap with considerable variability.[1,2] Clinical observation of the stretch reflexes also helps,[3] although it falls short of objectively evaluating the briskness, velocity, or symmetry. The use of a special hammer, which triggers the sweep on contact, allows recording of the electrical counterpart, the T reflex, which enhances its diagnostic yield by quantitating the response.

As might be predicted from studies of the H reflex in the hand and leg muscles,[4] a voluntary contraction of the target muscle should improve the consistency of the T-reflex recordings by increasing the excitability of the corresponding alpha

No commercial party having a direct financial interest in the results of the research supporting this article has or will confer a benefit on the authors or on any organization with which the authors are associated.

0003-9993/13/$36 - see front matter © 2013 by the American Congress of Rehabilitation Medicine
http://dx.doi.org/10.1016/j.apmr.2012.09.003

motoneurons through descending volitional inputs.[5,6] A background contraction also reduces the response variability by "clamping" motoneuron excitability at a standard level.[7] The use of an averaging technique defines the reflex latencies by differentiating the time-locked responses from randomly discharging motor unit activities.[8,9] These principles help standardize T-reflex testing in a wide variety of axial and limb muscles for clinical use.[10-12]

The present study attempts to establish a normative range of variability of the T reflexes elicited by a standardized method, and to verify its diagnostic utility in patients with unilateral CR.

Methods

We studied 160 limbs from 80 healthy subjects (50 men) evenly distributed across decades of age from 21 to 79 years (mean, 43y), and 12 consecutive patients (8 men) aged 40 to 75 years (mean, 53y) seen in our institute from November 2005 through September 2006 with an established diagnosis of CR involving a single root. All subjects agreed in writing to participate in the study after reading an informed consent.

A special rubber reflex hammer was constructed for triggering the sweep on contact with a piece of copper tape placed at the tip.[11,12] To standardize the strength of the blow of a tap delivered manually, the hammer contained a sensor[a] for detection of peak acceleration at the moment of contact. The value was displayed in the bar graph indicator of a light-emitting diode with peak hold circuit, allowing the examiner to adjust the blows close to a level of 8*g* (78m/s^2), ranging from 5.3 to 10.6*g*. Taps falling outside this level of strength were automatically rejected, triggering no sweep (fig 1).

T reflexes were recorded with subjects seated comfortably on an adjustable armchair in a quiet room. A pair of disk electrodes (NE-132B[b]), 11mm in diameter, was placed over the motor point of the target muscle as an active electrode and on the tendon or the neighboring bone as a reference electrode. The skin was prepared with an abrasive solution to reduce the impedance.

Voluntary background electromyographic activity of the muscle registered by these recording electrodes was simultaneously fed into a real-time integrating electromyographic analyzer,[c] detailed previously.[13] In short, the device served to quantify the isometric muscle tension by electromyographic waveform rectification followed by integration with a sampling rate of 640 per second. A digital readout of the integral for voluntary electromyographic activity to the nearest 500ms, displayed every 100ms, allowed the subject to adjust the force to 10% to 20% of the maximum effort (see fig 1).

The test muscles consisted of the biceps brachii (BB), the brachioradialis (BR), the triceps brachii (TB), and the first dorsal interosseous muscle (FDI) for C5, C6, C7, and C8 nerve root functions[14] (fig 2). An evoked response analyzer (Neuropack MEB-9100[b]) with a frequency response of 20Hz to 3kHz registered 2 traces to confirm consistency. Each test set comprised an average of 10 summated potentials for BB, BR, and TB, and 50 to 100 for FDI.

List of abbreviations:

BB biceps brachii
BR brachioradialis
CR cervical radiculopathy
FDI first dorsal interosseous muscle
MRI magnetic resonance imaging
TB triceps brachii

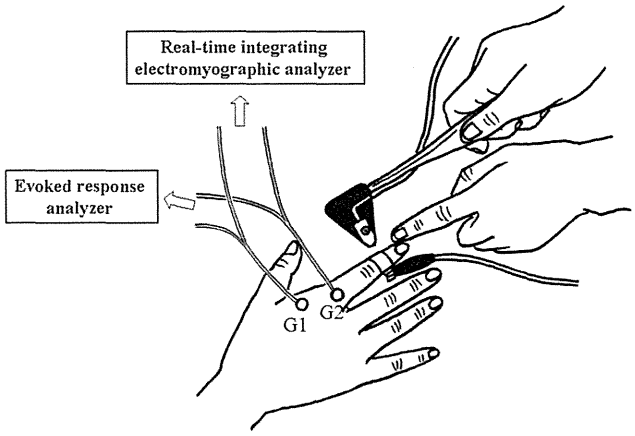

Fig 1 Schematic drawing of the T-reflex recording from the voluntarily contracted FDI. Mechanical taps were applied to the distal interphalangeal joint of the index finger using a special rubber reflex hammer with a piece of copper tape placed at the tip for triggering the sweep on contact with the copper tape placed on the tapping site. Electromyographic activity registered by a pair of disk electrodes was fed into both an evoked response analyzer for the T-reflex recording and a real-time integrating electromyographic analyzer for quantifying background voluntary electromyographic activity.

We measured onset latency and negative peak amplitude from the baseline and calculated side-to-side latency difference and amplitude ratio, dividing the smaller response by the larger response in healthy subjects, and the affected side by the unaffected side in patients.

Values were given as mean ± SD for statistical analyses by SPSS software,[d] considering $P<.05$ as significant.

Results

Normal T-reflex values

In 80 healthy subjects, standardized mechanical taps elicited T reflexes 100% of the time for BB and BR, 97% for TB, and 95% for FDI. Measurements (mean ± SD) included (1) right- and left-sided onset latencies of 16.1±1.7ms and 16.1±1.7ms for BB, 20.7±1.6ms and 20.5±1.6ms for BR, 17.1±1.6ms and 17.0±1.5ms for TB, and 32.6±3.8ms and 32.5±3.8ms for FDI; and (2) right- and left-sided amplitudes of 699±363μV and 684±358μV for BB, 247±158μV and 260±150μV for BR, 412±215μV and 427±255μV for TB, and 200±125μV and 179±88μV for FDI. Statistical analyses showed no difference ($P>.05$) in latency and amplitude between the 2 sides (table 1).

As expected, the T latency had a significant correlation with arm span and age for BB ($r=.46$ and .44), BR ($r=.41$ and .54), TB ($r=.56$ and .21), and FDI ($r=.42$ and .37) (all $P<.0001$) (table 2). Arm span was measured using a tape measure from one end of the tip of the middle finger to the other with the subjects' arms extended sideways at 90°.

Analyses using a simultaneous multiple regression line for arm span and age yielded the following formulas for T latency,

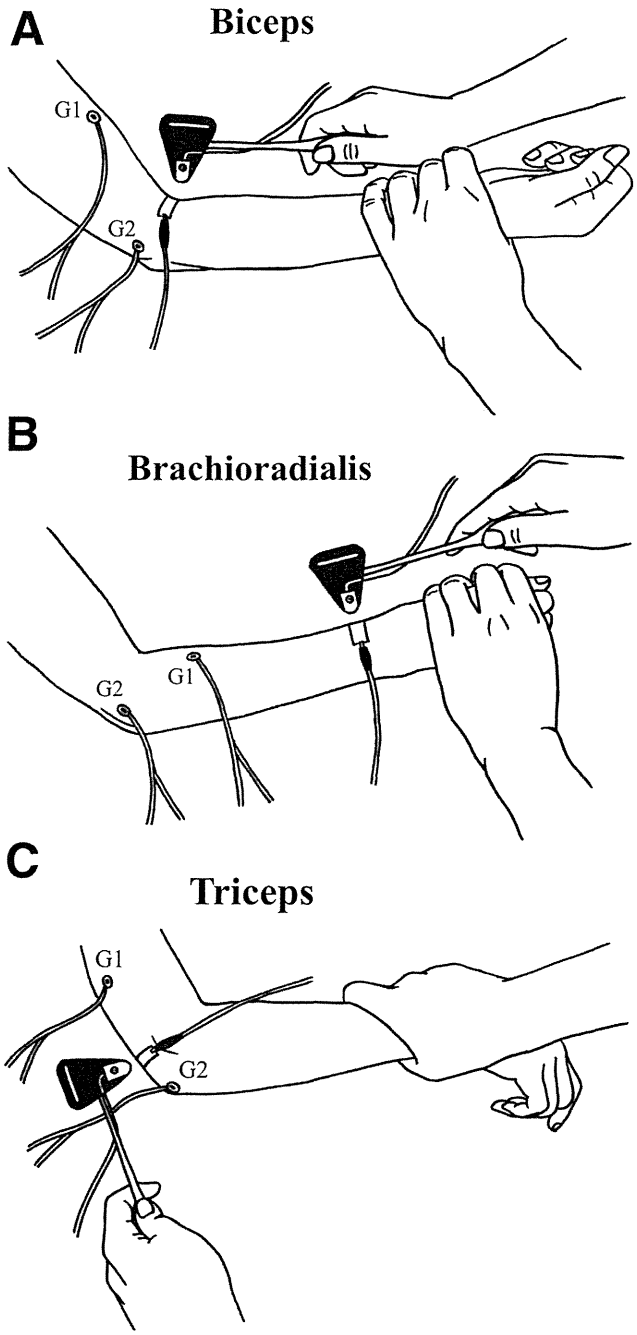

Fig 2 T-reflex studies of the BB (A), the BR (B), and the TB (C) evoked by muscle stretch induced by mechanical taps to the respective tendons. The recording leads consist of an active electrode (G1) placed over the motor point of the target muscle and a reference electrode (G2) placed over the lateral epicondyle of the humerus for the BB and the BR, and the olecranon for the TB.

showing a higher correlation coefficient than using a single variable (all $P<.0001$):

- BB T-latency = .05 × age (y) + .10 × arm span (cm) + 2.34 ($R=.68$)
- BR T-latency = .05 × age + .09 × arm span + 4.36 ($R=.72$)
- TB T-latency = .03 × age + .10 × arm span + .52 ($R=.62$)
- FDI T-latency = .09 × age + .20 × arm span + 4.05 ($R=.61$).

Based on a 95% confidence interval, the upper limits of the values predicted from age and arm span are as follows:

- BB T-latency = .06 × age + .08 × arm span + 1.43
- BR T-latency = .06 × age + .07 × arm span + 7.66
- TB T-latency = .04 × age + .08 × arm span + 3.09
- FDI T-latency = .12 × age + .15 × arm span + 4.94.

Calculation based on side-to-side latency differences (mean ± SD) in 80 healthy subjects—0.4±0.4ms (range, 0–1.7ms) for BB, 0.3±0.3ms (range, 0–1.6ms) for BR, 0.4±0.4ms (range, 0–1.4ms) for TB, and 0.5±0.6ms (range, 0–3.8ms) for FDI—yielded the following upper limits, defined as the mean + 2 SDs: 1.2ms for BB, 0.9ms for BR, 1.2ms for TB, and 1.7ms for FDI (see table 1).

Similarly, calculation based on side-to-side amplitude ratios, dividing the smaller by the larger T-reflex amplitude—82%±14% (range, 48%–100%) for BB, 71%±19% (range, 23%–100%) for BR, 74%±19% (range, 31%–100%) for TB, and 76%±16% (range, 36%–100%) for FDI—yielded the following lower limits, defined as the mean − 2 SDs: 54% for BB, 33% for BR, 36% for TB, and 44% for FDI (see table 1).

T-reflex study in patients

All 12 patients had a unilateral single cervical root lesion based on clinical symptomatology, magnetic resonance imaging (MRI) evidence of root compression, or diagnostic block of selective nerve root sheath injected with local anesthetic under fluoroscopic guidance. Weakness of upper limb muscles in a myotomal distribution helped localize the root lesion in 7 patients. MRIs revealed a distinct disk herniation or foraminal stenosis with a varying degree of disk bulge in 6 patients each. Selective nerve root block inducing substantial but temporary relief of pain delineated the root involved in 7 patients. Altogether, 2 patients had a C5 root lesion; 3, a C6 root lesion; 5, a C7 root lesion; and 2, a C8 root lesion (table 3).

The T reflex was either unelicitable or delayed in latency on the affected side in all patients. Table 3 summarizes latency, latency difference, and amplitude ratio in individual patients. Side-to-side comparison also showed latency differences or amplitude ratios outside the normative limits in all but 1 patient. In 2 patients with a C5 lesion, the BB reflex showed a latency difference of 2.6ms and 9.2ms, and an amplitude ratio of 29% and 63%. In 3 patients with a C6 lesion, the BR reflex showed a latency difference of 6.6ms, 2.6ms, and 3.1ms, and an amplitude ratio of 50%, 99%, and 45%. One of these patients also showed a TB reflex abnormality with a latency difference of 2.4ms (case 5). In 4 of 5 patients with a C7 lesion, the TB reflex showed latency differences ranging from 1.7 to 3.5ms (except for case 8 in which the TB reflex was unelicitable), and amplitude ratios from 0% to 30% (fig 3). In the remaining patient, the TB reflex revealed no side-to-side abnormalities (case 6). In 2 patients with a C8 lesion, the FDI reflex showed a latency difference of 8.1ms and an amplitude ratio of 42% in 1 patient and an absent response in the other (see table 3).

Collectively, analyses of side-to-side comparison in all 12 patients revealed a sensitivity of 92%, a specificity of 81%, and an accuracy of 83%. Corresponding values were 100%, 70%, and 75% for a C5 lesion by the BB reflex; 100%, 78%, and 83% for a C6 lesion by the BR reflex; 80%, 71%, and 75% for a C7 lesion

Table 1 T-reflex data for 80 healthy subjects

Measurement	BB	BR	TB	FDI
Latency (ms)				
R	16.1±1.7	20.7±1.6	17.1±1.6	32.6±3.8
L	16.1±1.7	20.5±1.6	17.0±1.5	32.5±3.8
Difference*	0.4±0.4 (1.2†)	0.3±0.3 (0.9†)	0.4±0.4 (1.2†)	0.5±0.6 (1.7†)
Amplitude (μV)				
R	699±363	247±158	412±215	200±125
L	684±358	260±150	427±255	179±88
Ratio (%)‡	82±14 (54§)	71±19 (33§)	74±19 (36§)	76±16 (44§)

NOTE. Values are mean ± SD or as otherwise indicated.
Abbreviations: L, left; R, right.
* Side-to-side latency difference.
† Upper limits of normal, calculated as the mean + 2SDs.
‡ Side-to-side amplitude ratios dividing the smaller T reflex by the larger response × 100.
§ Lower limits of normal, calculated as the mean − 2SDs.

by the TB reflex; and 100%, 100%, and 100% for a C8 lesion by the FDI reflex.

Discussion

Over the past 20 years, only a few studies have dealt with the diagnostic value of T reflexes recorded from the upper limb muscles. Schott and Koenig[15] originally reported the usefulness of the BB and the TB reflexes in unilateral cervical lesions. Kuruoglu and Oh,[16] studying healthy subjects, reported an inability to consistently elicit the T reflex from the TB, unlike the soleus and the rectus femoris reflexes elicitable in every subject. Pereon et al[17] also studied healthy subjects using a hammer fitted with a spring switch–triggered device. In this method, the inertial force of a built-in microswitch and the elastic compliance of the rubber cause a delay in triggering the sweep after impact. This, in turn, shortens the T-reflex latencies by as much as 4ms compared with a direct hammer–skin (strictly speaking, copper to copper) contact triggering system used in the present study.[11,12] More recently, with this externally triggered hammer–skin contact setup, Baker[18] reported a T reflex from the flexor digitorum profundus evoked by tapping the thenar eminence as a novel C8 stretch reflex.

In contrast to previous studies conducted with the test muscles at rest, we elicited T reflexes during voluntary contraction at 10% to 20% maximal effort to improve consistency. A real-time integrating electromyographic analyzer was used to standardize the degree of facilitation. The device automatically rectifies and integrates the voluntary electromyographic waveform registered by the same electrodes used to record the T reflex, and displays the normalized value of the integral every 100ms. Although the electromyographic signal–force relationship is not as linear in the BB as in the FDI,[19,20] the device nonetheless provided an easy way of maintaining a steady muscle contraction during the procedure.

In our setup, a mechanical tap externally triggers the sweep on hammer–skin contact,[11,18] which obviates the inertial force–related delay and the time variability of a built-in microswitch in triggering a sweep (see fig 1). Therefore, T-reflex latencies measured by this method slightly exceeded the values previously reported. The use of voluntary facilitation probably had no major effects on the T-reflex latencies, as evidenced in the H-reflex study of the flexor carpi radialis with the muscles relaxed or contracted.[7] In this case, the voluntary contraction should be of mild to moderate strength because strong contractions significantly alter the stiffness of tendon and muscle and, thereby, the degree of stretch rendered to the spindle endings.[11]

We have chosen 4 target muscles to assess the functional integrity of roots from C5 to C8 on the assumption that the BB is predominantly innervated by C5 and C6, the BR by C6, the TB by C7, and the FDI by C8 and T1.[14] Instead of the BR, the pronator teres or the extensor carpi radialis may serve for testing C6 root function.[1,21-25] A C8 reflex recently reported by Baker[18] was not used in the present study because this reflex is more complex in

Table 2 T-reflex latencies according to age group

	T-Reflex Latency (MS)			
Age Group (y)	BB	BR	TB	FDI
20–29	15.2±1.6 (N=30)	19.7±1.5 (N=30)	16.6±1.8 (N=30)	30.6±2.6 (N=30)
30–39	15.7±0.9 (N=11)	20.4±1.1 (N=11)	16.9±1.1 (N=11)	32.7±2.1 (N=11)
40–49	16.9±1.5 (N=9)	20.7±1.2 (N=9)	17.6±1.2 (N=9)	34.7±6.8 (N=9)
50–59	16.7±1.0 (N=10)	20.6±0.9 (N=10)	17.1±1.7 (N=10)	32.8±2.3 (N=9)
60–69	16.4±1.0 (N=10)	21.4±1.5 (N=10)	16.9±1.0 (N=9)	34.5±2.8 (N=8)
70–79	17.7±2.3 (N=10)	22.5±1.3 (N=10)	18.3±1.3 (N=9)	34.5±3.9 (N=10)

NOTE. Values are mean ± SD or as otherwise indicated.

Table 3 Clinical and T-reflex data for 12 patients with a single cervical root lesion

Case No.	Age (y)/Sex	Affected Root	MRI*	Root Block†	Muscles of MMT ≤4‡	T Reflex									
						Latency on Affected Side (ms)			Side-to-Side Latency Difference (ms)			Side-to-Side Amplitude Ratio (%)			
						BB	BR	TB	FDI	BB	BR	TB	FDI	BB	BR	TB	FDI
1	52/M	L–C5	Stenosis	N	DEL, BB	18.5§	22.5	17.3	35.9	2.6§	0.3	0	−0.6	29§	94	108	97
2	73/M	L–C5	Stenosis	N	DEL, BB	29.1§	27.8§	20.4	37.5	9.2§	0	0	−0.8	63	43	60	116
3	40/F	L–C6	Hernia	N	WRE	12.6	23.1§	14.4	24.8	0	6.6§	−0.1	0.1	104	50	114	54
4	44/M	L–C6	Hernia	Y	None	16.3	21.3§	17.6	32.3	0.1	2.6§	0.2	1.2	102	99	43	64
5	46/F	R–C6	Hernia	Y	None	13.9	21.7§	17.7	27.4	0.2	3.1§	2.4§	0.2	62	45	37	106
6	42/F	L–C7	Hernia	Y	TRIC, EDC	13.7	19.8	17.9§	28.6	0.5	0	0.7	−0.1	51§	119	36	96
7	47/M	R–C7	Hernia	Y	TRIC	17.7	21.1§	20.6§	34.1	0.9	2.7§	1.7§	−0.3	40§	36	29§	89
8	57/M	L–C7	Hernia	Y	None	16.5	21.2	NR	34.3	0	0	NR	0.5	80	77	0§	97
9	52/F	L–C7	Stenosis	Y	None	15.7	18.3	20.7§	30.8	0.4	0.1	2.0§	−0.6	79	44	29§	100
10	65/M	L–C7	Stenosis	N	None	15.9	21.5	18.8§	37.0	0	1.1§	3.5§	−0.5	79	60	30§	92
11	45/M	R–C8	Stenosis	N	EDC, intrinsics	16.8	20.8	20.6§	40.5§	0.3	0	0.8	8.1§	242	62	40	42§
12	75/M	L–C8	Stenosis	Y	EDC, intrinsics	19.2	24.3	19.6§	NR	1.4§	0.4	0.2	NR	82	99	19§	0§

Abbreviations: DEL, deltoid; EDC, extensor digitorum communis; F, female; M, male; MMT, manual muscle testing; N, no; NR, not recordable; TRIC, triceps; WRE, wrist extensors; Y, yes.

* MRI finding of either a distinct disk herniation or foraminal stenosis.

† Patients who underwent selective nerve root block to determine the root responsible for the radicular pain.

‡ Muscles of a distinct weakness with MMT.

§ Values outside the normative limits.

that it depends on the synaptic connections between primary afferent fibers from the flexor pollicis longus and motor neurons innervating the heteronymous muscles (the long finger flexors, etc). Instead, we tested the FDI as a C8-innervated muscle,[1,21,22,24] which is frequently involved in C8 nerve root compression.[26]

The T-reflex latencies, as expected, showed a high correlation with age and arm span in healthy subjects, which enabled a simultaneous regression analysis to predict the upper limits of normative values adjusted to these 2 functions. In assessing a unilateral lesion, a comparison of the 2 sides generally provides the most sensitive measure of the T or H reflex recorded from the soleus.[2,27] The same principle applies to our data, which revealed high sensitivity (92%) and specificity (81%) despite myotomal overlaps, in assessing a unilateral single cervical root lesion. In particular, T-reflex studies helped evaluate the patients with the sole complaint of upper limb pain as in cases 4, 5, 8, 9, and 10 (see table 3 and fig 3). In addition to side-to-side latency comparison, absolute latency values often exceeded the upper limit predicted from age and arm span. Thus, by inference, this method can also serve as a diagnostic measure for bilateral cervical lesions.

Our study confirms the clinical value of the standardized T reflex in assessing axon loss and motor and IA afferents conduction abnormalities.[28] Viewed in this light, T reflexes, which assess both afferent and efferent pathways, complement needle electromyography to improve the electrodiagnosis of cervical root lesions, which rarely affect the motor fibers selectively.[1] Noninvasive T-reflex testing has an advantage over an invasive procedure of selective nerve root block to verify the root of interest for surgical intervention. In the clinical domain, the practical usefulness of this test would be if it can localize the radicular lesions in the patients who have neither motor nor sensory deficits on physical examination, nor abnormalities on needle electromyography. This point requires further study on a group of such patients.

Study limitations

There are some limitations to our study. First, T-reflex latencies and amplitudes were measured by 1 investigator, so that interobserver agreement was not confirmed. Second, electromyography was performed in only a few patients who agreed to have a needle study, which precluded the comparison between T-reflex and electromyographic values in assessing a unilateral single cervical root lesion. Third, we developed a special reflex hammer that contained a sensor which standardizes the strength of the blow of a tap delivered manually. This device, however, is not commercially available at the moment, which may partially preclude other investigators from reproducing our technique. This study nonetheless contributes toward reassessment of the potentially useful T reflex as an electrodiagnostic technique.

Conclusions

Based on the data in 80 healthy subjects, the present study established a normative range of variability of the T reflexes elicited from the BB (C5), BR (C6), TB (C7), and the FDI (C8) during standardized volitional contraction monitored by a real-time integrating electromyographic analyzer. Comparison of the T-reflex latencies and amplitudes between the 2 sides localized the C5 to C8 solitary root lesions in 12 patients with a high sensitivity (92%), specificity (81%), and accuracy (83%). In addition to side-to-side comparison, the absolute latency values of the T reflexes, if

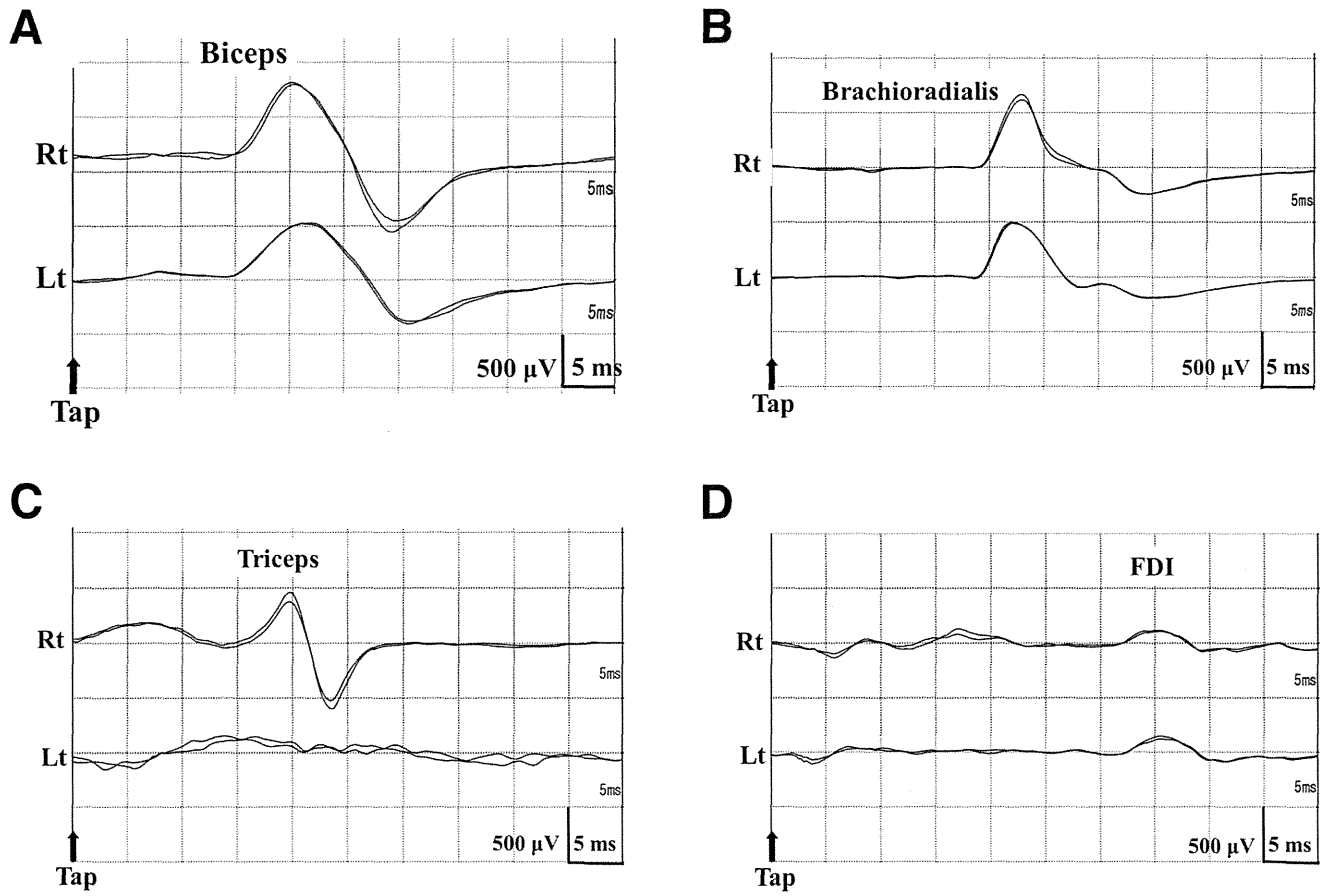

Fig 3 The T reflexes recorded bilaterally from the BB (A), BR (B), TB (C), and FDI (D) in a 57-year-old patient with left C7 radiculopathy (case 8). Selective C7 nerve root block under fluoroscopic guidance inducing substantial relief of pain helped localize the root lesion, although the patient had no weakness or wasting of upper limb muscles to aid in diagnosis. Side-to-side comparison of the T reflexes showed latency differences or amplitude ratios within the normative limits for all responses except for the triceps reflex, which was unelicitable on the affected side.

elicitable, on the affected side exceeded the upper limit predicted from age and arm span in all patients.

Suppliers

a. EFP-G02B01; Matsushita Electronic Components, 1006 Kadoma, Osaka, 571-8501, Japan.
b. Nihon Kohden, 1-31-4 Nishiochiai, Tokyo, 161-8560 Japan.
c. EBS-SK1; Ebisu Denki Co Ltd, 266-3 Takaoka-cho, Tosa, 781-1103, Japan.
d. SPSS version 16.0; SPSS Inc, 19-21 Hakosaki-cho, Tokyo, 103-8510, Japan.

Keywords

Radiculopathy, cervical; Reflex, stretch; Rehabilitation; Upper extremity

Corresponding author

Tomoko Tetsunaga, MD, Dept of Orthopaedic Surgery, Kochi Medical School, Kohasu Oko-cho, Nankoku 783-8505, Japan. *E-mail address:* kwdtmk1201@yahoo.co.jp.

References

1. Wilbourn AJ, Aminoff MJ. AAEE minimonograph #32: the electrophysiologic examination in patients with radiculopathies. Muscle Nerve 1988;11:1099-114.
2. Kimura J. Electrodiagnosis in diseases of nerve and muscle: principles and practice. 3rd ed. New York: Oxford University Pr; 2001. p 628-49.
3. Wainner RS, Fritz JM, Irrgang JJ, Boninger ML, Delitto A, Allison CS. Reliability and diagnostic accuracy of the clinical examination and patient self-report measures for cervical radiculopathy. Spine 2003;28:52-62.
4. Hagbarth KE. Post-tetanic potentiation of myotatic reflexes in man. J Neurol Neurosurg Psychiatry 1962;25:1-10.
5. McComas AJ, Sica REP, Upton ARM. Excitability of human motoneurones during effort. J Physiol 1970;210:145-6.
6. Upton ARM, McComas AJ, Sica REP. Potentiation of 'late' responses evoked in muscles during effort. J Neurol Neurosurg Psychiatry 1971; 34:699-711.
7. Burke D, Adams RW, Skuse N. The effects of voluntary contraction on the H reflex of human limb muscles. Brain 1989;112:417-33.
8. Trontelji JV, Pecak F, Dimitrijevic MR. Segmental neurophysiological mechanism in scoliosis. J Bone Joint Surg Br 1979;61: 310-3.
9. Eisen A, Burton K, Larsen A, Hoirch M, Calne D. A new indirect method for measuring spinal conduction velocity in man. Electroencephalogr Clin Neurophysiol 1984;59:204-13.

10. Tani T, Kimura J, Nakazumi Y, Yamamoto H. Mechanically and electrically evoked long-latency responses in the human thenar muscle during voluntary contraction. Jpn J Electroencaphalogr Electromyogr 1991;19:40-8.
11. Tani T, Yamamoto H, Ichimiya M, Kimura J. Reflexes evoked in human erector spinae muscles by tapping during voluntary activity. Electroencephalogr Clin Neurophysiol 1997;105:194-200.
12. Tani T, Kida K, Yamamoto H, Kimura J. Reflexes evoked in various human muscles during voluntary activity. In: Shimoji K, Kurokawa T, Tamaki T, Willis WD, editors. Spinal cord monitoring and electrodiagnosis. Berlin Heidelberg: Springer-Verlag; 1991. p 226-36.
13. Ishida K, Tani T. Development of portable real-time EMG integrator. Chubuseisaisi 2003;46:1113-4.
14. Hoppenfeld S. Physical examination of the spine and extremities. New York: Appleton-Century-Crofts; 1976. p 118-25.
15. Schott K, Koenig E. T-wave response in cervical root lesions. Acta Neurol Scand 1991;84:273-6.
16. Kuruoglu R, Oh SJ. Quantitation of tendon reflexes in normal volunteers. Electromyogr Clin Neurophysiol 1993;33:347-51.
17. Pereon Y, Tich SNT, Fournier E, Genet R, Guiheneuc P. Electrophysiological recording of deep tendon reflexes: normative data in children and in adults. Neurophysiol Clin 2004;34:131-9.
18. Baker SK. Characterization of a novel C8 phasic muscle stretch reflex. Muscle Nerve 2009;40:529-34.
19. Milner-Brown HS, Stein RB. The relation between the surface electromyogram and muscular force. J Physiol 1975;246:549-69.
20. Lawrence JH, DeLuca CJ. Myoelectric signal versus force relationship in different human muscles. J Appl Physiol 1983;54:1653-9.
21. Delagi EF, Perotto A, Iazzetti J, Morrison D. Anatomic guide for the electromyographer. 2nd ed. Springfield: CC Thomas; 1981. p 4-76.
22. Katirji MB, Agrawal R, Kantra TA. The human cervical myotomes: an anatomical correlation between electromyography and CT/myelography. Muscle Nerve 1988;11:1070-3.
23. Levin KH, Maggiano HJ, Wilbourn AJ. Cervical radiculopathies: comparison of surgical and EMG localization of single-root lesions. Neurology 1996;46:1022-5.
24. Kimura J. Electrodiagnosis in diseases of nerve and muscle: principles and practice. 3rd ed. New York: Oxford University Pr; 2001. p 466-94.
25. Rainville J, Noto DJ, Jouve C, Jenis L. Assessment of forearm pronation strength in C6 and C7 radiculopathies. Spine 2007;32: 72-5.
26. Wallace D. Disc compression of the eighth cervical nerve: pseudo ulnar palsy. Surg Neurol 1982;18:295-9.
27. Braddom RI, Johnson EW. Standardization of H reflex and diagnostic use in S1 radiculopathy. Arch Phys Med Rehabil 1974;55:161-6.
28. Miller TA, Pardo R, Yaworski R. Clinical utility of reflex studies in assessing cervical radiculopathy. Muscle Nerve 1999;22:1075-9.

J. Spine Res. 4 : 116-122, 2013

Original Article

Risk Factors for Development of Myelopathy in Patients with Asymptomatic Ossification of the Posterior Longitudinal Ligament

Shunji Matsunaga[*1], Takashi Tsuji[*2], Yoshiaki Toyama[*2], Kosei Ijiri[*3], Setsuro Komiya[*3], Takuya Numasawa[*4], Satoshi Toh[*4], Shoichi Ichimura[*5], Kazuhiro Satomi[*5], Atsushi Seichi[*6], Yuichi Hoshino[*6], Katsushi Takeshita[*7], Kozo Nakamura[*7], Kenji Endo[*8], Kengo Yamamoto[*8], Yoshiharu Kato[*9], Takeshi Kato[*10], Kenichi Shinomiya[*10], Yasuaki Tokuhashi[*11], Yoshiharu Kawaguchi[*12], Tomoatsu Kimura[*12], Yukihiro Matsuyama[*13], Naoki Ishiguro[*14], Masashi Neo[*15], Takashi Nakamura[*15], Takahito Fujimori[*16], Motoki Iwasaki[*16], Hideki Yoshikawa[*16], Shinichiro Taniguchi[*17], Toshikazu Tani[*17], Yoshihiko Kato[*18], Toshihiko Taguchi[*18], Kimiaki Sato[*19], Kensei Nagata[*19]

[*1]Department of Orthopaedic Surgery, Imakiire General Hospital
[*2]Department of Orthopedic Surgery, School of Medicine, Keio University
[*3]Graduate School of Medical and Dental Sciences, Kagoshima University
[*4]Department of Orthopaedic Surgery, Hirosaki University Graduate School of Medicine
[*5]Department of Orthopaedic Surgery, Kyorin University School of Medicine
[*6]Department of Orthopedics, Jichi Medical University
[*7]Departments of Orthopaedic Surgery, Faculty of Medicine, The University of Tokyo
[*8]Department of Orthopedic Surgery, Tokyo Medical University
[*9]Department of Orthopedic Surgery, Tokyo Women's Medical University
[*10]Department of Orthopedic Surgery, Tokyo Medical and Dental University
[*11]Department of Orthopedic Surgery, Nihon University School of Medicine
[*12]Department of Orthopaedic Surgery, Faculty of Medicine, University of Toyama
[*13]Department of Orthopaedic Surgery, Hamamatsu University School of Medicine
[*14]Department of Orthopaedic Surgery, Nagoya University Graduate School of Medicine
[*15]Department of Orthopaedic Surgery, Graduate School of Medicine, Kyoto University
[*16]Department of Orthopaedic Surgery, Osaka University Graduate School of Medicine
[*17]Department of Orthopaedic Surgery, Kochi Medical School, Kochi University
[*18]Department of Orthopaedic Surgery, Yamaguchi University Graduate School of Medicine
[*19]Department of Orthopaedic Suegery, Kurume University School of Medicine

Author for correspondence : Shunji Matsunaga MD, PhD, Department of Orthopaedic Surgery, Imakiire General Hospital(4-16 Shimotatsuo chou, Kagoshima, Japan 892-8502)
Received July 24, 2012, accepted November 2, 2012

Abstract

A multi-center study was designed to clarify the course of future neurological deterioration in patients with asymptomatic ossification of the posterior longitudinal ligament (OPLL). A total of 109 asymptomatic subjects with OPLL from 17 spine institutes nationwide were followed for an average of 11.3 years. Factors related to development of myelopathy were investigated by logistic regression analysis. A total of 27/109 (24.8%) subjects developed myelopathy during follow-up. All patients with greater than 60% spinal canal stenosis in the plain radiographs developed myelopathy. The range of motion of the cervical spine was significantly larger in patients with myelopathy than in those without it. The patients with less than 60% spinal canal stenosis who developed myelopathy without cervical trauma history had lateral deviated-type OPLL in 94% of cases. These risk factors for development of myelopathy in subjects with asymptomatic OPLL presented by this study should be considered when asymptomatic subjects with OPLL were followed conservatively.

Key words : ossification of the posterior longitudinal ligament (OPLL), cervical spine, maximum spinal canal stenosis, computed tomography, axial ossified pattern, logistic regression analysis

INTRODUCTION

Ossification of the posterior longitudinal ligament (OPLL) is a hyperostotic condition of the spine associated with severe neurological deficits[1-2]. Myelopathy in patients with OPLL is generally considered to be caused by compression of the spinal cord due to ossification of the ligaments. However, some patients with large OPLL do not exhibit myelopathy for a long period of time[3]. In contrast, some patients with relatively small OPLL exhibit myelopathy[4]. The pathomechanism of the development of myelopathy in patients with OPLL remains unclear. It is difficult to predict the course of future neurological deterioration in patients with asymptomatic OPLL. We have designed a multi-center cohort study to identify the predictors of the development of myelopathy in patients with OPLL.

SUBJECTS AND METHODS

A total of 109 OPLL patients (66 male and 43 female) from 17 spine institutes nationwide enrolled in this study. Retrospective chart review was performed to form a cohort study. All subjects met the following criteria for enrollment : (1) radiographic evidence of OPLL in the cervical spine, (2) asymptomatic OPLL at the initial examination associated with a minimum five years follow-up, and (3) agreement from the patients and approval from each institutional review board to use clinical data for this study. The term "asymptomatic" was defined as indicating that the patients did not exhibit apparent myelopathy. Evidence of myelopathy was determined by subjective and objective findings including spastic gait, muscle atrophy, weakness, motor dysfunction of the hand, abnormal tendon reflex of the upper and lower extremities, pathological reflexes, clonus and sensory disturbances by direct examination. All subjects with myelopathy had disabilities affecting their daily lives. Subjects who had stiffness of the neck and a limited range of motion of the cervical spine were included in this study. All subjects had yearly clinical examination at each spine institutes. Age at the first visit of subjects ranged from 41 to 84 with an average of 59.8 years old. OPLL was classified into three types according to the Japanese Ministry of Health, Labour and Welfare[5] : segmental, 33 cases ; continuous, 38 cases ; and mixed 38 cases. The follow-up periods ranged from 5 to 26 years (mean 11.3 years). The clinical characteristics of enrolled subjects are summarized in Table 1. Each subject underwent plain radiograph, CT, and MRI of the

Table 1 Clinical characteristics of enrolled subjects

Number of institutes	17
Number of subjects	109
Gender	Male : 66 ; Female : 43
Age at the first visit(yr)	41-84(mean 59.8)
Follow-up periods(yr)	5-26(mean 11.3)
OPLL type*	
Segmental type	33
Continuous type	38
Mixed type	38

*Classification by the Investigation Committee on the ossification of the posterior longitudinal ligaments of the Japanese Ministry of Public Health, Labour and Welfare

cervical spine at the initial examination. The range of motion (ROM) of the cervical spine was determined by using flexion-extension plain radiographs. The angle between C1 and the inferior margin of C7 was measured on a plain radiographs. The ROM was estimated as the total of angles of maximum flexion position and maximum extension position. Myelopathy-free rate during the follow-up periods was calculated by Kaplan-Meier method[6]. The trauma history of the cervical spine, gender, age at first examination, OPLL type on plain radiograph, length of follow-up period, maximum percentage of spinal canal stenosis in plain radiograph, ROM of the cervical spine, and axial ossified pattern in MRI or CT were reviewed in relation to the development of myelopathy in these asymptomatic OPLL patients during follow-up. The measurement and classification of ossification type were performed by three radiologists with blind review of clinical data.

Statistical analysis

ROM was compared between myelopathy group and non-myelopathy group by the Student t-test. To investigate the association between myelopathy group and other factors, multiple logistic regression analysis was performed. These analyses were performed using SAS Release 9.2 (SAS Institute Inc., Cary, NC, USA.). A significance level of 0.05 was used for all statistical tests.

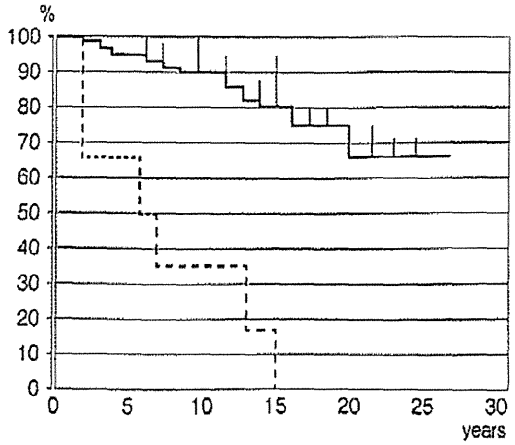

Figure 1 Myelopathy-free rate of asymptomatic subjects with OPLL by the Kaplan-Meier method. The bold line indicates the data of subjects with less than 60% spinal canal stenosis. The dotted line indicates the data of subjects with greater than 60% spinal canal stenosis.

RESULTS

A total of 27/109 (24.8%) subjects developed myelopathy during follow-up. The remaining 82 patients did not exhibit myelopathy throughout the follow-up periods with a minimum of 5 years. Six of 27 subjects who exhibited myelopathy had trauma history. Of the 6 subjects, 5 had mixed-type OPLL, and one had segmental-type OPLL. The types of trauma reported included three falls on stairs, two severe whiplash injuries, and one accidental head contusion. All five patients with greater than 60% spinal canal stenosis in the plain radiograph developed myelopathy within 15 years of follow-up. The myelopathy-free rate was shown by the Kaplan-Meier method (Figure 1). The myelopathy-free rate of subjects with less than 60% spinal canal stenosis was 66% at the maximum 26 years of follow-up. Among the 104 subjects with less than 60% spinal canal stenosis, ROM of the cervical spine in subjects with myelopathy was significantly larger than that in those without it (Table 2). On the basis of CT and MRI, the axial ossified pattern could be classified into two types : central and lateral deviated. The determination

Table 2 The range of motion of the cervical spine in 104 subjects with less than 60% spinal canal stenosis

Factor	Development of myelopathy (22 subjects)	Not development of myelopathy (82 subjects)	p Value
ROM (degree)	58.8 ± 10.2	37.2 ± 12.5	0.008

Results are expressed as mean ± standard deviation
ROM : range of motion of the cervical spine measured by the plain X-ray film

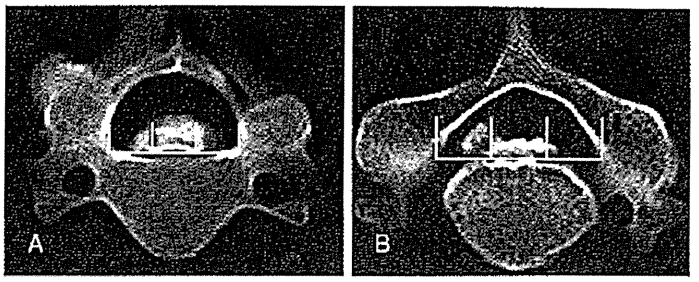

Figure 2 Classification of the axial ossification pattern on CT examination.
A : central-type B : lateral deviated-type
The lines indicate that width of vertebra canal is divided into three equal parts.

of the types is explained as follows. The central-type was defined as that in which the most occupied portion of OPLL was located within the middle one third of the width of the vertebral canal on the axial CT or MRI (Figure 2A). The lateral deviated-type was defined as that in which the most occupied portion of OPLL was located outside middle one third of the width (Figure 2B). Among 98 subjects with less than 60% spinal canal stenosis without trauma history, the lateral deviated-type OPLL was found in 48 cases, and the central-type OPLL was found in 50 cases. The subjects who developed myelopathy and without cervical a trauma history had lateral-deviated type OPLL in 94% (15/16) of the cases. The subjects who did not develop myelopathy had lateral-deviated type OPLL in 40% (33/82) of the cases. The sensitivity of lateral deviated-type OPLL for development of myelopathy was 94% and the specificity was 60%.

Age at the initial examination, gender, classification of OPLL, history of trauma on the cervical spine, maximum spinal canal stenosis, range of motion of the cervical spine, and axial ossification type on CT or MRI were analyzed using univariate and multivariate logistic models to investigate the association with the development of myelopathy in asymptomatic subjects with OPLL. From results of univariate logistic regression analysis, the significant risk factors for myelopathy were OPLL type (mixed and continuous type), large ROM of the cervical spine, lateral-deviated type OPLL on CT, and maximum spinal canal stenosis ratio (Table 3). Multivariate logistic regression analysis revealed the same results as univariate analysis (Table 4). Probabilities of myelopathy predicted by the multivariate logistic regression model had 87% accuracy to observed myelopathy data.

DISCUSSION

All published research on the relationship between the occurrence of myelopathy and radiographic findings was performed by single research center using plain radiographs of the cervical spine. Our study was

Table 3 The results of univariate logistic regression analysis of the development of myelopathy

Factor		Development of Myelopathy		Crude Odds Ratio		
		Yes	No	OR	95% Wald CI	P-value
Gender	Male	18(27.7)	47(72.3)			
	Female	9(20.5)	35(79.5)	0.671	0.270-1.671	0.3920
Age (yrs)	<65	18(32.1)	38(67.9)			
	>=65	9(17.0)	44(83.0)	0.432	0.174-1.073	0.0706
	Mean±SD	59.6±8.6	61.3±9.1	0.979	0.932-1.028	0.3960
Type of OPLL	Segmental	4(12.1)	29(87.9)			
	Mixed	18(47.4)	20(52.6)	6.536	1.919-22.222	0.0002
	Continuous	5(13.2)	33(86.8)	1.099	0.269-4.484	0.1405
Trauma History	Negative	21(21.9)	75(78.1)			
	Positive	6(46.2)	7(53.8)	3.062	0.929-10.095	0.0660
ROM (degree)	<50	7(17.9)	32(82.1)			
	>=50	20(28.6)	50(71.4)	1.829	0.694-4.816	0.2219
	Mean±SD	55.4±12.9	44.7±12.9	1.082	1.033-1.135	0.0010
Axial OPLL type	Central	8(14.8)	46(85.2)			
	Lateral deviated	19(34.5)	36(65.5)	3.035	1.192-7.723	0.0198
Maximum Canal Stenosis (%)	<60	22(21.2)	82(78.8)			
	>=60	5(100.0)	0(0.0)	-	-	
	Mean±SD	45.6±11.1	38.4±10.8	1.062	1.018-1.109	0.0054

ROM : range of motion of the cervical spine, SD : standard deviation, OR : odds ratio, CI : confidence interval

Table 4 The results of multivariate logistic regression analysis of the development of myelopathy

Factor			Analysis of Maximum Likelihood Estimates				Odds Ratio	
			DF	Estimate	SE	Wald ChiSq	P-value	Estimate	95% Wald CI
Intercept		β_0	1	-17.003	3.682	21.325	<.0001		
Type of OPLL	Mixed	β_1	1	1.004	0.444	5.108	0.0238	3.863	0.641-23.269
	Continuous	β_2	1	-0.656	0.517	1.614	0.2039	0.734	0.099-5.462
ROM(degree)		β_3	1	0.153	0.040	14.566	0.0001	1.165	1.077-1.260
Axial OPLL type	Lateral deviated	β_4	1	1.001	0.405	6.119	0.0134	7.396	1.515-36.101
Maximum Canal Stenosis(%)		β_5	1	0.186	0.047	15.716	<.0001	1.205	1.099-1.321

ROM : range of motion of the cervical spine, DF : degree of freedom, SE : standard error, ChiSq : Chi-Squared, CI : confidence interval

designed as a nationwide multi-center study based on definite inclusion criteria.

Matsunaga et al examined the natural course of 450 OPLL patients with an average of 17.6 years of follow-up[7]. Myelopathy was originally identified in 127 patients, and 55(17%) of the remaining 323 patients without original myelopathy exhibited myelopathy during the follow-up interval. The authors reported that all OPLL patients with a residual spinal canal less than 6mm developed myelopathy during follow-up[3]. Harsh et al reported that the critical level of the residual spinal canal for the development of myelopathy in

patients with OPLL was 9mm[8]. However, the measurement of the residual spinal canal depended on the X-ray tube-film distance and this distance was not the same in all studies. It has been reported that all OPLL patients with 60% or greater maximum stenosis of the spinal canal as a result of ossified ligaments exhibited myelopathy regardless of the history of cervical trauma[9]. On the basis of postmortem examinations, Kameyama et al reported that irreversible cord damage developed in patients with 40% or greater maximum stenosis of the spinal canal[10]. The static compression factor of the spinal cord seems to be a radiographic predictor of the development of myelopathy. The presented study revealed that spinal canal stenosis greater than 60% in a plain radiograph was a risk factor for the development of myelopathy in OPLL.

OPLL patients with less than 60% spinal canal stenosis, dynamic factors should be considered for the occurrence of myelopathy. A large range of motion of the cervical spine was a risk factor for the development of myelopathy. Similarly, Morio et al also previously noted the existence of dynamic factors related to the development of myelopathy in patients with OPLL[11].

Severe myelopathy can be induced by cervical trauma in patients with OPLL. However, previous study revealed a low incidence of trauma-induced myelopathy in patients with OPLL by a long-term follow up[9]. In the current study, only six subjects developed myelopathy by cervical trauma. We could not determine the risk factor for trauma-induced myelopathy because of a limited number of cases.

On the basis of CT and MRI examinations, we classified the axial view OPLL pattern into two types : central and lateral deviated. The former retrospective study also revealed that the patients with lateral deviated-type OPLL developed myelopathy more frequently than the patients with central-type OPLL[12]. In this study, subjects with less than 60% spinal canal stenosis who developed myelopathy without cervical trauma history had lateral deviated-type OPLL in 94% (15/16) of the cases. We could not determine why patients with lateral deviated-type OPLL exhibited significantly higher myelopathy than patients with central-type OPLL. Biomechanical factors for the spinal cord might influence the pathomechanism. The distribution of strain into the spinal cord is different in the central-type compression to lateral deviated-type compression. The impairment of the neurological tract might be different as a result of the compression pattern of the spinal cord.

The risk factors for development of myelopathy in subject with asymptomatic OPLL were proposed by the current logistic regression analysis. The accuracy of this analysis was 87% and we might predict development of myelopathy by checking the radiographic risk factors. We think that this study can give useful information on management of subjects with asymptomatic OPLL. However, we could not determine whether cervical trauma is a risk factor of development of myelopathy or not. This is limitation of the current study and we need further prospective study for large number of patients to determine the risk factors for development of myelopathy in subjects with asymptomatic OPLL.

Acknowledgement

This study was performed with the aid of the Investigation Committee on the Ossification of the Spinal Ligaments of the Japanese Ministry of Health, Labour and Welfare. This study was performed with the approval of the Clinical Research Ethics Committee of each institute.

References

1) Ono K, Ota H, Tada K, et al : Ossified posterior longitudinal ligament : a clinicopathologic study. Spine. 1997 ; 2 : 126-138
2) Tsuyama N : Ossification of the posterior longitudinal ligament of the spine. Clin Orthop Relat Res. 1984 ; 184 : 71-84
3) Matsunaga S, Kukita M, Hayashi K, et al : Pathogenesis of myelopathy in patients with ossification of the posterior longitudinal ligament. J Neurosurg (2 Suppl). 2002 ; 96 : 168-172
4) Nose T, Egashira T, Enomoto T et al : Ossification of the